

## Materials and Methods

### *Hepatic proteomics analysis*

As there was no statistically significant difference in steatosis phenotypes between male and female mice (Figures 1A and B), four mice were randomly selected from each group (i.e., control and fructose) for the proteomics analysis. Protein fractions were isolated using harvested liver tissues from the experiment I. In brief, approximately 50 mg of liver was rinsed with 4 mL of PBS twice and then 800  $\mu$ L of PBS was added; liver tissues were then homogenized with a plastic disposable pestle. Typically, 10-12 gentle strokes were sufficient to homogenize the tissues. Isolated proteins were reduced, alkylated, and digested using filter-aided sample preparation as described elsewhere <sup>1</sup>. Tryptic peptides were then labeled with a tandem mass tag 6-plex isobaric label reagent set (Thermo Scientific) followed by fractionation on a 100  $\times$  1.0 mm Acquity BEH C18 column (Waters, Milford, MA) using an UltiMate 3000 UHPLC system (Thermo Scientific); a total of 36 fractions were then consolidated into six super-fractions. The resulting six super fractions were further separated by reverse phase XSelect CSH C18 2.5  $\mu$ m resin (Waters) on an in-line 120  $\times$  0.075 mm column using an UltiMate 3000 RSLCnano system (Thermo Scientific). Eluted peptides were ionized by electrospray (2.15 kV) followed by mass spectrometric analysis on an Orbitrap Fusion Tribrid mass spectrometer (Thermo Scientific) using multi-notch MS3 parameters as described <sup>2</sup>. Mass spectrometer data were acquired in top-speed profile mode at a resolution of 240,000 over a range of 375 to 1500 m/z. After collision induced dissociation activation (normalized collision energy of 35), MS/MS data were acquired using the ion trap analyzer in centroid mode over a range of 400-2000 m/z. Up to 10 MS/MS precursors were selected for higher energy collision dissociation activation (normalized collision energy of 65.0), followed by MS3 reporter ion data acquisition in profile mode at a resolution of

30,000 over a range of 100-500 m/z. Proteins were identified and reporter ions quantified using the MaxQuant software (Max Planck Institute, Munchen, Germany) with a parent ion tolerance of 3 ppm, a fragment ion tolerance of 0.5 Da, and a reporter ion tolerance of 0.03 Da. Results were compiled using Scaffold program (Proteome Software, Portland, OR), and protein identifications were accepted in which false discovery was less than 1% and at least two identified peptides were contained. The data of protein detections were transformed to  $\log_2$  values; resulting normalized values were used to make a short-list. The proteins showing  $p$  value  $< 0.05$  and fold change  $> 1.5$  were considered significantly different; the resulting 179 differentially expressed proteins (DEPs) were then subjected to the Ingenuity Pathway Analysis (IPA) software (Qiagen, Hilden, Germany).

#### *Measurement of mRNA expression*

Liver tissues were lysed using the QIAzol Lysis Reagent Kit (Qiagen) and then total RNA was isolated using the RNeasy Mini Kit (Qiagen). Quality control for extracted total RNA was monitored using conventional A260/280 ratio and A260/230 ratio methods (NanoDrop 2000 Spectrophotometer; Thermo-Fisher Scientific). After, 2  $\mu\text{g}$  of total RNA was reverse transcribed utilizing the High Capacity cDNA Reverse Transcription Kit (Applied Biosystems, Foster City, CA) per the manufacturer's protocol. Expressions of mRNAs were measured by quantitative reverse transcription PCR (qPCR) analysis using the ABI 7500 system (Applied Biosystems) in a reaction mixture containing TaqMan Gene Expression Master Mix, primers tagged with TaqMan probe, and cDNA. PCR amplification was conducted under the following conditions: one cycle at 50°C for 2 min and 95°C for 10 min, followed by 40 cycles of denaturation (95°C for 15 s) and annealing (60°C for 1 min). Genes of interest were normalized with a reference gene,  $\beta$ -

*actin*. Data were analyzed with 7500 Software (Ver. 2.1; Applied Biosystems) using the  $2^{-\Delta\Delta CT}$  method. Detailed primer information is provided in Online Supplementary Table 2. All samples were run in triplicate.

#### *Measurement of mature miRNA expression*

Total RNA was isolated as described above. Ten nanograms of isolated RNA was utilized to synthesize cDNA using TaqMan MicroRNA Reverse Transcription Kit (Applied Biosystems). MicroRNA-specific cDNA was amplified with respective specific primers. Detailed miRNA primer information is provided in Online Supplementary Table 2. Expression of the mature miRNAs was measured by qPCR analysis using the ABI 7500 system (Applied Biosystems). A 20  $\mu$ L of qPCR reaction included 2 $\times$  Universal PCR Master Mix (10  $\mu$ L), 10 $\times$  TaqMan microRNA Expression Assay (1  $\mu$ L), and miRNA-specific cDNA (2  $\mu$ L). PCR amplification was conducted under the conditions described above. Genes of interest were normalized to that of reference genes, snoRNA-202 for tissue and miR-16 for serum. Data were analyzed with 7500 Software (Ver. 2.1; Applied Biosystems) using the  $2^{-\Delta\Delta CT}$  method. All samples were run in triplicate.

#### *Measurement of protein expression*

Protein expression was assessed using western blotting. Detailed primary antibody information is provided in Online Supplementary Table 3. In brief, protein samples (1 mg/mL) were dissolved in 1 $\times$  sample buffer and then heated for 10 min to denature proteins. After, the samples were separated via SDS-PAGE and then transferred to a nitrocellulose membrane. Membranes were blocked in blocking buffer containing 5% BSA in Tris-buffered saline (0.5 M

Tris base, 9% NaCl, and 1% Tween 20; pH 7.8) for 1 h followed by incubation with primary antibodies for 12 h at 4°C. The membranes were then incubated with the HRP conjugated secondary antibodies for 1 h at room temperature. The protein bands were detected using the ImageQuant LAS 4000 (GE Healthcare Life Sciences, Marlborough, MA) and their intensity was quantified using ImageJ software (NIH, Bethesda, MD). Each membrane included a reference sample, which is used in all blots, and the final results were calculated as the ratio of protein/ $\beta$ -actin divided by the ratio of the reference sample/ $\beta$ -actin to factor in inter-assay variation.

### *Histological analyses*

Liver tissues were fixed in 10% neutral buffered formalin in PBS (wt:vol) and then embedded in Tissue-Tek Optimal Cutting Temperature compound (Sakura Finetek, Torrance, CA). Tissues were cut into 10  $\mu$ m sections and stained with Oil Red O (ORO) and Hematoxylin and Eosin (H&E) staining for lipid accumulation and morphological observations, respectively. Stained liver sections were examined using 20 $\times$  for H&E staining or 40 $\times$  for ORO staining objective on a Leica DM 500 microscope equipped with a Leica ICC50E (Leica Camera Inc., Wetzlar, Germany), and then quantified using ImageJ software (NIH).

### *Measurement of serum aspartate aminotransferase and alanine aminotransferase levels*

The levels of aspartate aminotransferase (AST) and alanine aminotransferase (ALT) in serum were measured using Cobas c-111 biochemical analyzer (Roche, Basel, Switzerland)<sup>3</sup>. The experiment was performed according to the manufacturer's instruction.

### *Determination of hepatic ferroptosis*

Formalin fixed and paraffinized liver tissues were utilized for Perls' Prussian blue staining described elsewhere <sup>4</sup>. Tissue sections were deparaffinized and rehydrated with gradient ethanol treatment. Subsequently, tissue section slides were incubated with 5% potassium ferrocyanide in 1.13 M HCl solution overnight at room temperature. After rinsing the slides with distilled water twice for 2 min, the tissue slides were incubated with methanol containing 0.01 M sodium azide and 0.3% hydrogen peroxide for 1 h at room temperature. Then, the tissue sections were rinsed with 0.1 M PBS thrice for 2 min, and incubated in a mixture containing 0.025% 3,3'-Diaminobenzidine-4HCl (DAB) and 0.005% hydrogen peroxide in 0.1 M PBS pH 7.4 for 30 min. After rinsing the slides thrice with distilled water for 2 min, the slides were counterstained with nuclear fast red for 5 min, followed by dehydration, and mounting with permanent mounting medium. Pictures were taken using 40× objective on a Leica DM 500 microscope equipped with a Leica ICC50E (Leica Camera Inc.). DAB positive area was quantified using IHC profiler plugin function in ImageJ Software (NIH).

### *Measurement of lipid peroxidation*

Markers for lipid peroxidation were assessed. Expression of 4-hydroxynonenal (4-HNE) was assessed by immunofluorescence in the liver tissues. Briefly, formalin fixed and paraffinized liver tissues were utilized. Deparaffinized and rehydrated tissues were incubated in citrate buffer (10 mM citric acid, 0.05% Tween 20, pH 6.0), and microwaved for 2 min for antigen retrieval. Then, tissue sections were permeabilized with 0.2% triton-X100 for 10 min. After rinsing the tissue sections with PBS, tissue sections were blocked with normal goat serum for 30 min at room temperature, followed by incubation with anti-4-HNE antibody (1:100 diluted in normal

goat serum) for 12 h at 4°C. Subsequently, the tissue sections were rinsed with PBS and incubated with fluorophore-conjugated secondary antibody (1:200 dilution in photobleaching media) for 30 min at room temperature, followed by mounting tissues with mount media. The nuclei of the tissue were counterstained with 4',6-diamidino-2-phenylindole (DAPI) and images were visualized and captured by fluorescence microscope (Carl Zeiss AG). Malondialdehyde (MDA) level in the liver tissues was examined by western blotting.

#### *In vitro fructose treatment*

Mouse liver normal cell line (AML12; CRL-2254; American Type Culture Collection, Manassas, VA) was maintained in DMEM/F12 media (American Type Culture Collection) supplemented with 10% fetal bovine serum, 40 ng/mL dexamethasone, Insulin-Transferrin-Selenium-G Supplement (Invitrogen, Carlsbad, CA). Cultures were maintained at 37°C with 5% CO<sub>2</sub> and water saturation. When the culture was 80%-90% confluent, the cells were split. Cell culture media was changed three times per week. To validate the experiment I, 50 mM fructose was treated to cells for 72 h to induce liver cell toxicity and to examine its effect on miR-33 and protein expression levels. Afterwards, the cells were harvested for further analyses (i.e., qPCR and western blot).

#### *In vitro validation of miRNA-mRNA interactions*

AML12 was treated with mimics or inhibitors of miR-33-5p (miR-33 hereafter), or scramble oligos (Thermo-Fisher Scientific). Ten micromolar mimics, inhibitors, or scramble were transfected using Lipofectamine RNAiMAX Transfection Reagent (Thermo-Fisher Scientific), as directed by manufacturer's instructions. The AML12 cells were harvested 72 h

after transfection for western blotting and qPCR analyses to validate interactions between miRNAs and predicted target genes.

### *Statistical analyses and bioinformatic analyses*

A sample size calculation for the experiment I was calculated based on our previous report; effect size of 0.55,  $\alpha$  error probability of 0.05, and power (1- $\beta$  error probability) of 0.8<sup>5</sup>. For the experiment II, we referred to results from the experiment I. Since miR-33 expression (in response to fructose intake) is the major dependent variable, hepatic miR-33 expression data was utilized to calculate an effect size (i.e., 0.69). The effect size of 0.69,  $\alpha$  error probability of 0.05, and power (1- $\beta$  error probability) of 0.8 were subjected to the G\*Power software (University of Düsseldorf, Düsseldorf, Germany) to determine the total sample size for the experiment II. As a result, the total sample size required was 24 (8 mice per group).

Data were expressed as means  $\pm$  standard deviation (SD). All data associated with the experiment I were analyzed by two tailed, Welch's *t* test for unequal variance correction. A *p* value of 0.05 or less was considered statistically significant (GraphPad Prism Version 7.00; GraphPad Software, Inc., San Diego, CA). For the time-course or dose-dependent effect, one-way ANOVA test was performed. Tukey's multiple comparison or Dunnett's multiple comparisons test was performed for each time or dose to distinguish each effect.

For bioinformatic analysis, the DEPs, generated based on the criteria described above was subjected to the IPA software. In the IPA software, Canonical Pathways or Disease and Biofunctions were used via the Core Analysis feature with *p* values calculated using the Fisher's Exact test. Further, the Upstream Analysis was performed in order to find upstream regulator(s)

of proteins that are differentially expressed by the fructose intervention. To predict potential interactions between proteins and miRNAs, manual literature searches, software-, and web server-based target searches were conducted using the PubMed, IPA knowledge-based database, and TargetScan 7.1 ([www.targetscan.org](http://www.targetscan.org)). MicroRNAs targeting the top upstream regulator were retrieved from the PubMed, IPA software, and the TargetScan database. In addition, miRNAs influenced by fructose intervention in rodent models were selected. Overlapped miRNAs in the two different searches (i.e., upstream regulator targeting miRNAs and miRNAs influenced by fructose intervention) were selected as candidate miRNAs for further processes.

Supplemental Table 1. Composition of AIN-93G purified diet

Diet ingredients	AIN-93G
Cornstarch, g	398
Dextrinized cornstarch, g	132
Casein, g	200
Sucrose, g	100
Cellulose, g	50.0
Mineral mix <sup>1</sup> , g	35.0
Vitamin mix <sup>2</sup> , g	10.0
L-Cystine, g	3.00
Choline bitartrate, g	2.50
Soybean oil <sup>3,4</sup> , g	70.0
Total, kg	1.00

<sup>1</sup>AIN-93G mineral mix.

<sup>2</sup>AIN-93G vitamin mix.

<sup>3</sup>The antioxidant, t-butylhydroquinone (0.02% wt:vol) was included in soybean oil.

<sup>4</sup>Specific gravity of soybean oil is 0.920

Supplemental Table 2. A list of TaqMan primers

Primer	Manufacturer	Catalog number	RefSeq
For mRNA expressions			
$\beta$ -actin ( <i><math>\beta</math>-actin</i> )		Mm02619580_g1	NM_007393.5
Acetyl CoA Carboxylase- $\alpha$ ( <i>Acaca</i> )		Mm01304257_m1	NM_133360.2
Fatty Acid Synthase ( <i>Fasn</i> )	Life Technologies	Mm00662319_m1	NM_007988.3
Stearoyl-CoA Desaturase-1 ( <i>Scd1</i> )		Mm00772290_m1	NM_009127.4
Sterol Regulatory Element Binding Protein 1 ( <i>Srebpl</i> )		Mm00550338 m1	NM 011480.3
For miRNA expressions			Accession number
snoRNA202		001232	AF357327
mmu-miR-122-5p		002245	MIMAT0000246
mmu-miR-125b-1-3p		002378	MIMAT0004669
mmu-miR-130a-3p	Life Technologies	000454	MIMAT0000141
mmu-miR-16-5p		000391	MIMAT0000527
mmu-miR-19b-3p		000396	MIMAT0000513
mmu-miR-33-5p		465396_mat	MIMAT0000667

Supplemental Table 3. A list of primary antibodies

Antibody	Manufacturer	Catalog number
Anti-Acetyl CoA Carboxylase (ACC)	Cell Signaling Technology	3662
Anti-Actin	Cell Signaling Technology	4970
Anti-Fatty Acid Synthase (FAS)	Cell Signaling Technology	3180
Anti-Glutathione (GSH)	Virogen	101-A
Anti-Malondialdehyde (MDA)	Abcam	ab6463
Anti-Sterol Regulatory Element-Binding Protein 1 (SREBP-1)	Santa Cruz Biotechnology	SC-365513
Anti-Stearoyl-CoA Desaturase-1 (SCD1)	Cell Signaling Technology	2794
Anti-4-Hydroxynonenal (4-HNE)	Abcam	ab46545

Supplemental Table 4. Effects of fructose on daily body weight, food intake, water intake, calorie intake, and serum parameters<sup>1</sup>

	Control	Fructose
Initial body weight, g	17.43 ± 0.53	17.43 ± 0.56
Final body weight, g	23.07 ± 0.58	23.45 ± 0.57
Body weight gain <sup>2</sup> , g	5.65 ± 0.22	6.02 ± 0.17
Food intake, g/day/mouse	2.84 ± 0.17	1.75 ± 0.09**
Water intake, g/day/mouse	6.90 ± 0.17	11.01 ± 0.25***
Calorie intake <sup>3</sup> , kcal/day/mouse	10.80 ± 0.27	20.39 ± 0.14***
Total Cholesterol, mg/dL	86.65 ± 2.13	99.85 ± 2.78**
HDL Cholesterol, mg/dL	57.18 ± 1.80	56.60 ± 1.82
LDL Cholesterol, mg/dL	7.53 ± 0.38	10.83 ± 1.02*
Triacylglyceride, mg/dL	20.3 ± 2.93	30.18 ± 2.36*
Glucose, mg/dL	176.48 ± 6.57	293.80 ± 12.27***

<sup>1</sup>All results are expressed as means ± SEM. <sup>2</sup>Final body weight – Initial body weight. <sup>3</sup>Total calorie intake was calculated based on calorie contributions of diet and fructose (3.8 kcal/g·AIN-93G and 3.67 kcal/g·fructose). Control, AIN-93G group; Fructose, fructose intervention group (34% fructose in deionized water, wt:vol). \* indicates statistically significant (\**p* < 0.05; \*\**p* < 0.01; \*\*\**p* < 0.001). No statistical difference was found in initial body weight, final body weight, body weight gain, and liver tissue weight between Control and Fructose groups.

Supplemental Table 5. A list of differentially expressed proteins<sup>1</sup> in proteomics dataset of mice liver tissues

Protein	Fold change vs. Control
AGXT	-8.41
CYP4F14	-3.69
CYP2C50	-3.48
ARG1	-3.13
HAL	-3.05
CYP2C54	-2.95
CYP2A5	-2.94
HSD17B2	-2.90
GLS2	-2.76
PIGR	-2.64
CTH	-2.57
SQOR	-2.51
SULT1B1	-2.45
ASS1	-2.38
CYP1A2	-2.34
CYP2C23	-2.33
CYP3A25	-2.33
CML1	-2.32
MAOB	-2.28
CML2	-2.25
BHMT	-2.24
HSD17B13	-2.24
CYP7A1	-2.22
METTL7A1	-2.15
CYP2E1	-2.15
CYB5A	-2.12
INF2	-2.11
PON1	-2.09
ETHE1	-2.07
RAB21	-2.04
SLC6A12	-2.04
METTL7B	-2.02
CPS1	-1.99
SLC25A15	-1.97
IIGP1	-1.95
SFXN2	-1.92
KMO	-1.90
SLC22A18	-1.90
POR	-1.89

---

FECH	-1.88
CA14	-1.87
HSD3B3	-1.87
PXMP2	-1.85
PRODH2	-1.83
TMEM126B	-1.81
CYP51A1	-1.80
SARAF	-1.80
CDO1	-1.78
SLCO1A6	-1.78
OAT	-1.77
FDFT1	-1.76
MVK	-1.74
SUGCT	-1.74
RAPGEF4	-1.73
IGTP	-1.69
TRIM14	-1.69
DBT	-1.69
RDH10	-1.67
PRODH	-1.67
SUOX	-1.67
PHB2	-1.67
CYP3A13	-1.65
TMBIM6	-1.64
ETFRF1	-1.62
IFI47	-1.61
SLCO1A4	-1.60
ERGIC2	-1.59
TMEM256	-1.59
RHOT2	-1.59
DHCR24	-1.59
HSD17B11	-1.57
SLC25A22	-1.56
SCARB1	-1.55
TTPA	-1.55
FAAH	-1.55
TGM1	-1.53
MTCH1	-1.52
RAB43	-1.52
GJB2	-1.51
GPAM	1.50
BPNT1	1.51
FGA	1.52

---

---

---

SLC37A4	1.53
ARCN1	1.53
GARS	1.53
HRG	1.55
EIF5A	1.55
MYO6	1.55
PRDX1	1.55
KYNU	1.56
EIF3I	1.56
GSTM1	1.56
THA1	1.56
PYGB	1.57
YWHAH	1.58
VNN1	1.58
CSRP1	1.59
KHSRP	1.61
RRBP1	1.62
PRKAG1	1.63
FERMT2	1.63
RNH1	1.65
GPD1L	1.65
DSTN	1.65
CTSD	1.66
HNRNPL	1.68
PDHA1	1.69
ENPEP	1.71
CNDP2	1.71
EIF3D	1.71
CLTB	1.71
FLNB	1.72
SARS	1.73
TPI1	1.74
FGG	1.78
ALDOA	1.79
CORO1C	1.80
GYS2	1.81
CFL1	1.81
TIMM8B	1.81
TXNL1	1.81
EEF1B	1.86
CCT2	1.90
RPS10	1.92
STBD1	1.94

---

---

---

---

HAO1	1.97
ERH	1.98
TPM3	1.98
ACOT11	2.03
ACSS2	2.03
GM6793	2.03
EPN1	2.03
FDPS	2.04
TTR	2.05
GLUL	2.05
THNSL2	2.06
CORO1A	2.09
CMAS	2.10
PMM2	2.14
AGL	2.14
PARK7	2.15
LGALS1	2.16
PCYT2	2.19
SULT1C2	2.20
CS	2.20
ELOVL5	2.29
AACS	2.36
EIF2B3	2.40
KHK	2.41
FAM136A	2.44
GALK1	2.45
DBI	2.55
GPD2	2.55
ACACB	2.64
ENO1	2.64
MIF	2.92
GPD1	2.94
GLO1	3.05
ECHDC2	3.14
SCD1	3.18
GLRX5	3.25
TKFC	3.25
CSAD	3.33
NPM1	3.34
CMPK1	3.62
ELOVL6	3.68
ALDOB	4.17
UGP2	4.22

---

---

---

---

MYL12A	4.24
PGD	4.30
THRSP	4.73
FABP5	5.31
APOA4	5.31
NAT8F3	5.48
FASN	6.00
ACLY	6.20
PKLR	6.54
ME1	7.75
ACACA	7.94

---

---

<sup>1</sup> Proteins with Fold Change > ±1.5 and p < 0.05 were selected as differentially expressed proteins.

Supplemental Table 6. A complete list of miRNAs regulating *Srebf1*

miRNA	Species	Accession	Source
miR-1178-5p	Human	MIMAT0022940	
miR-1234-3p	Human	MIMAT0005589	
miR-128-1-5p	Human, Rat, Mouse	MIMAT0026477 (Human); MIMAT0017118 (Rat); MIMAT0016982 (Mouse)	
miR-1292-3p	Human	MIMAT0022948	
miR-149-3p	Human	MIMAT0004609	
miR-18a-5p	Human, Rat, Mouse	MIMAT0000072 (Human); MIMAT0000787 (Rat); MIMAT0000528 (Mouse)	
miR-3065-3p	Human, Rat, Mouse	MIMAT0015378 (Human); MIMAT0017840 (Rat); MIMAT0014837 (Mouse)	
miR-3070-5p	Human, Mouse	MIMAT0026475 (Human); MIMAT0014846 (Mouse)	
miR-3173-5p	Human, Mouse	MIMAT0019214 (Human); MIMAT0027883 (Mouse)	
miR-3177-3p	Human	MIMAT0015054	
miR-3181	Human	MIMAT0015061	
miR-328-5p	Human	MIMAT0026486	
miR-342-5p	Human, Rat, Mouse	MIMAT0004694 (Human); MIMAT0004652 (Rat); MIMAT0004653 (Mouse)	
miR-3612	Human	MIMAT0017989	IPA
miR-383-3p	Human	MIMAT0026485	database
miR-4327	Human	MIMAT0016889	
miR-4443	Human	MIMAT0018961	
miR-4459	Human	MIMAT0018981	
miR-4497	Human	MIMAT0019032	
miR-4665-3p	Human	MIMAT0019740	
miR-4695-5p	Human, Rat	MIMAT0019788 (Human); MIMAT0017370 (Rat)	
miR-4715-5p	Human	MIMAT0019824	
miR-532-3p	Human, Rat, Mouse	MIMAT0004780 (Human); MIMAT0005323 (Rat); MIMAT0004781 (Mouse)	
miR-5571-5p	Human	MIMAT0022257	
miR-6075	Human	MIMAT0023700	
miR-6749-5p	Human	MIMAT0027398	
miR-6768-5p	Human	MIMAT0027436	
miR-6801-3p	Human	MIMAT0027503	

miR-6825-3p	Human	MIMAT0027551	
miR-6886-5p	Human	MIMAT0027672	
miR-486-5p	Human, Rat, Mouse	MIMAT0002177 (Human); MIMAT0037265 (Rat); MIMAT0003130 (Mouse)	6
miR-219a-5p	Human, Rat, Mouse	MIMAT0000276 (Human); MIMAT0000889 (Rat); MIMAT0000664 (Mouse)	7
miR-192-5p	Human, Rat, Mouse	MIMAT0000222 (Human); MIMAT0000867 (Rat); MIMAT0000517 (Mouse)	8
miR-103-3p	Human, Rat, Mouse	MIMAT0000101 (Human); MIMAT0000824 (Rat); MIMAT0000546 (Mouse)	9
miR-33-5p	Human, Rat, Mouse	MIMAT0000091 (Human); MIMAT0000812 (Rat); MIMAT0000667 (Mouse)	10, 11
miR-27a-5p	Human, Rat, Mouse	MIMAT0004501 (Human); MIMAT0004715 (Rat); MIMAT0004633 (Mouse)	12

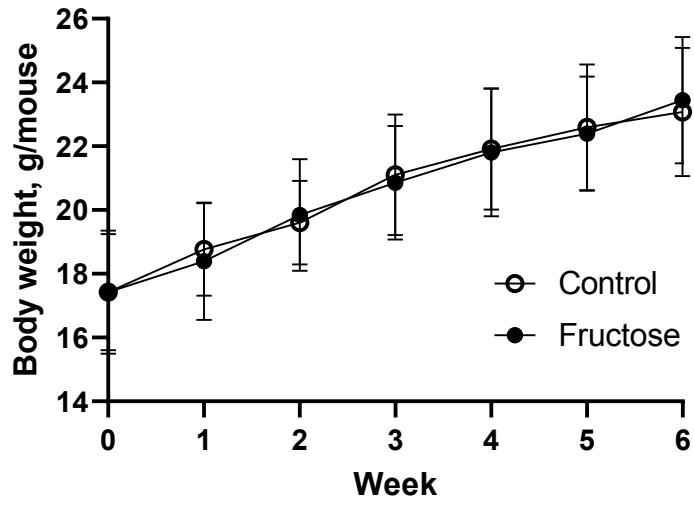
Supplemental Table 7. Expression of miR-33 in different species and experimental conditions

Direction of miR-33	Model/Location of expression	Detection method	Diet or disease or patient	Reference
<i>Increased</i>	Human/Liver	PCR <sup>1</sup>	Obese patients	13
<i>Increased</i>	Goose/Liver	PCR	Overfeeding carbohydrate diet	14
<i>Increased</i>	Rat/Liver	PCR	HFD <sup>3</sup>	15
<i>Decreased</i>	Mouse/Liver	PCR	HFD	16
<i>Increased</i>	Rat/Liver/PBMC <sup>3</sup>	PCR	Standard diet plus cafeteria diet	17
<i>Decreased</i>	Mouse/Liver	PCR	High fructose diet	18
<i>Decreased</i>	Mouse/Liver	PCR	HCD vs HFD	19
<i>Increased</i>	Rat/Liver/Blood	PCR	Soft pellet food vs hard pellet food	20
<i>Decreased</i>	Mouse/Liver	PCR	HFD	21
<i>Increased</i>	Rat/Liver	PCR	Lard oil	22

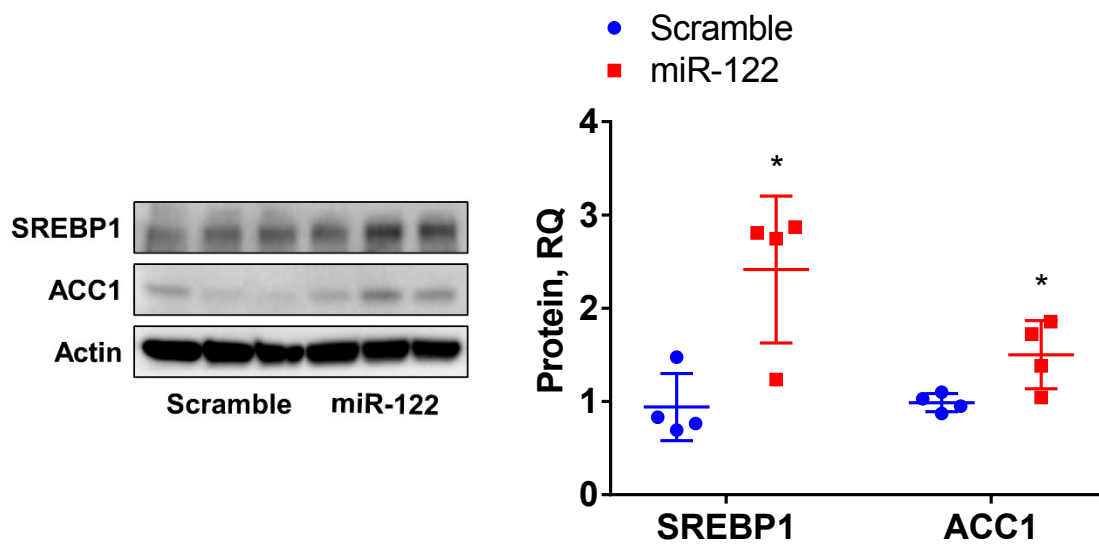
<sup>1</sup>quantitative RT PCR

<sup>2</sup>PBMC, peripheral blood mononuclear cell

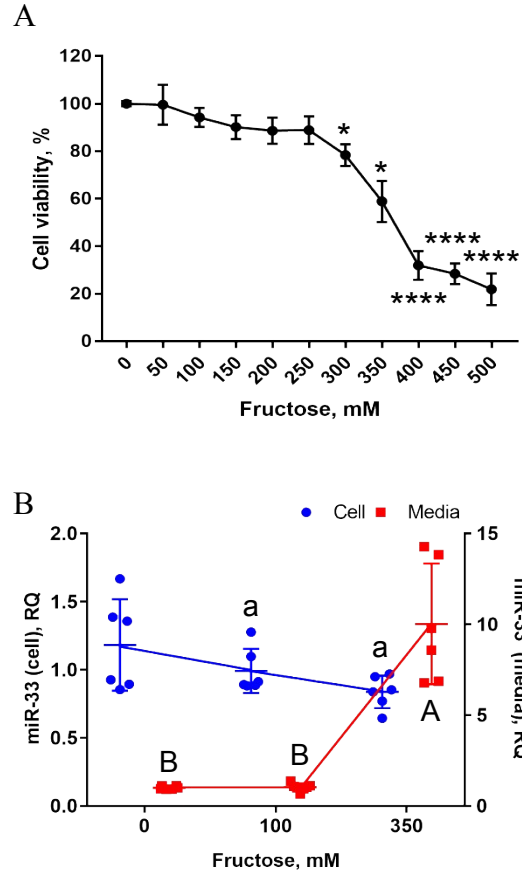
<sup>3</sup>HFD, high fat diet; HCD, high carbohydrate diet



Supplemental Figure 1. Effect of fructose on daily body weight. Daily body weight was measured every week on the same day and time (n=6). Values are means  $\pm$  SD.



Supplemental Figure 2. Effect of microRNA-122 transfection on SREBP1 and ACC1 protein expressions in AML12 hepatocytes. Values are means  $\pm$  SD (n=4). \*p < 0.05



Supplemental Figure 3. Effect of fructose on microRNA-33 in cell and growth media. (A) Changes in cell viability in AML12 cells treated with fructose were evaluated using MTT assay. Cells from 3 different cultures with triplicates of experimental replications were utilized for the analyses (n=3). Values are means  $\pm$  SD. \* $p < 0.05$ , \*\*\*\* $p < 0.0001$  (vs. 0 mM Fructose) (B) Dose-dependent effects of fructose on miR-33 expression were assessed using qPCR analysis in cells or cultured media. Cells from 3 different cultures with duplication of experimental replications were utilized for the analyses (n=3). Values are means  $\pm$  SD. Scatter plots with different letters represents statistically different at  $p < 0.05$ .

## References

1. J. R. Wisniewski, A. Zougman, N. Nagaraj and M. Mann, Universal sample preparation method for proteome analysis, *Nat. Methods*, 2009, **6**, 359-362.
2. G. C. McAlister, D. P. Nusinow, M. P. Jedrychowski, M. Wuhr, E. L. Huttlin, B. K. Erickson, R. Rad, W. Haas and S. P. Gygi, MultiNotch MS3 enables accurate, sensitive, and multiplexed detection of differential expression across cancer cell line proteomes, *Anal. Chem.*, 2014, **86**, 7150-7158.
3. J. L. Bowling and A. Katayev, An evaluation of the Roche Cobas c 111, *Lab. Med.*, 2010, **41**, 398-402.
4. S. van Duijn, R. J. Nabuurs, S. G. van Duinen and R. Natta, Comparison of histological techniques to visualize iron in paraffin-embedded brain tissue of patients with Alzheimer's disease, *J. Histochem. Cytochem.*, 2013, **61**, 785-792.
5. J. H. Pan, J. Tang, K. E. Beane, M. C. Redding, Y. J. Cho, Y. J. Kim, J. Zhao, E. C. Shin, J. H. Lee, B. C. Kong and J. K. Kim, Hepatic transcriptomics analysis reveals that fructose intervention down-regulated xenobiotics-metabolising enzymes through aryl hydrocarbon receptor signalling suppression in C57BL/6N mice, *Br. J. Nutr.*, 2019, **122**, 769-779.
6. L. S. Niculescu, N. Simionescu, E. V. Fuior, C. S. Stancu, M. G. Carnuta, M. D. Dulceanu, M. Raileanu, E. Dragan and A. V. Sima, Inhibition of miR-486 and miR-92a decreases liver and plasma cholesterol levels by modulating lipid-related genes in hyperlipidemic hamsters, *Molecular biology reports*, 2018, **45**, 497-509.
7. A. L. Moyano, J. Steplowski, H. Wang, K. N. Son, D. I. Rapolti, J. Marshall, V. Elackattu, M. S. Marshall, A. K. Hebert, C. R. Reiter, V. Ulloa, K. C. Pituch, M. I. Givogri, Q. R. Lu, H. L. Lipton and E. R. Bongarzone, microRNA-219 Reduces Viral Load and Pathologic Changes in Theiler's Virus-Induced Demyelinating Disease, *Molecular therapy : the journal of the American Society of Gene Therapy*, 2018, **26**, 730-743.
8. Y. Lin, D. Ding, Q. Huang, Q. Liu, H. Lu, Y. Lu, Y. Chi, X. Sun, G. Ye, H. Zhu, J. Wei and S. Dong, Downregulation of miR-192 causes hepatic steatosis and lipid accumulation by inducing SREBF1: Novel mechanism for bisphenol A-triggered non-alcoholic fatty liver disease, *Biochimica et biophysica acta*, 2017, **1862**, 869-882.
9. A. Gracia, A. Fernandez-Quintela, J. Miranda, I. Eseberri, M. Gonzalez and M. P. Portillo, Are miRNA-103, miRNA-107 and miRNA-122 Involved in the Prevention of Liver Steatosis Induced by Resveratrol?, *Nutrients*, 2017, **9**.
10. C. Fernandez-Hernando and K. J. Moore, MicroRNA modulation of cholesterol homeostasis, *Arteriosclerosis, thrombosis, and vascular biology*, 2011, **31**, 2378-2382.
11. T. Horie, T. Nishino, O. Baba, Y. Kuwabara, T. Nakao, M. Nishiga, S. Usami, M. Izuhara, N. Sowa, N. Yahagi, H. Shimano, S. Matsumura, K. Inoue, H. Marusawa, T. Nakamura, K. Hasegawa, N. Kume, M. Yokode, T. Kita, T. Kimura and K. Ono, MicroRNA-33 regulates sterol regulatory element-binding protein 1 expression in mice, *Nat Commun*, 2013, **4**, 2883.
12. T. Shirasaki, M. Honda, T. Shimakami, R. Horii, T. Yamashita, Y. Sakai, A. Sakai, H. Okada, R. Watanabe, S. Murakami, M. Yi, S. M. Lemon and S. Kaneko, MicroRNA-27a regulates lipid metabolism and inhibits hepatitis C virus replication in human hepatoma cells, *Journal of virology*, 2013, **87**, 5270-5286.

13. J. Vega-Badillo, R. Gutierrez-Vidal, H. A. Hernandez-Perez, H. Villamil-Ramirez, P. Leon-Mimila, F. Sanchez-Munoz, S. Moran-Ramos, E. Larrieta-Carrasco, I. Fernandez-Silva, N. Mendez-Sanchez, A. R. Tovar, F. Campos-Perez, T. Villarreal-Molina, R. Hernandez-Pando, C. A. Aguilar-Salinas and S. Canizales-Quinteros, Hepatic miR-33a/miR-144 and their target gene ABCA1 are associated with steatohepatitis in morbidly obese subjects, *Liver Int*, 2016, **36**, 1383-1391.
14. Y. Zheng, S. Jiang, Y. Zhang, R. Zhang and D. Gong, Detection of miR-33 Expression and the Verification of Its Target Genes in the Fatty Liver of Geese, *Int. J. Mol. Sci.*, 2015, **16**, 12737-12752.
15. H. Wang, Y. Shao, F. Yuan, H. Feng, N. Li, H. Zhang, C. Wu and Z. Liu, Fish Oil Feeding Modulates the Expression of Hepatic MicroRNAs in a Western-Style Diet-Induced Nonalcoholic Fatty Liver Disease Rat Model, *Biomed Res Int*, 2017, **2017**, 2503847.
16. P. Ghareghani, M. Shanaki, S. Ahmadi, A. R. Khoshdel, N. Rezvan, R. Meshkani, M. Delfan and S. Gorgani-Firuzjaee, Aerobic endurance training improves nonalcoholic fatty liver disease (NAFLD) features via miR-33 dependent autophagy induction in high fat diet fed mice, *Obes. Res. Clin. Pract.*, 2018, **12**, 80-89.
17. L. Baselga-Escudero, A. Arola-Arnal, A. Pascual-Serrano, A. Ribas-Latre, E. Casanova, M. J. Salvado, L. Arola and C. Blade, Chronic administration of proanthocyanidins or docosahexaenoic acid reverses the increase of miR-33a and miR-122 in dyslipidemic obese rats, *PLoS One*, 2013, **8**, e69817.
18. N. Sud, H. Zhang, K. Pan, X. Cheng, J. Cui and Q. Su, Aberrant expression of microRNA induced by high-fructose diet: implications in the pathogenesis of hyperlipidemia and hepatic insulin resistance, *J. Nutr. Biochem.*, 2017, **43**, 125-131.
19. X. Li, F. Lian, C. Liu, K. Q. Hu and X. D. Wang, Isocaloric Pair-Fed High-Carbohydrate Diet Induced More Hepatic Steatosis and Inflammation than High-Fat Diet Mediated by miR-34a/SIRT1 Axis in Mice, *Sci. Rep.*, 2015, **5**, 16774.
20. C. R. Bae, K. Hasegawa, S. Akieda-Asai, Y. Kawasaki, K. Senba, Y. S. Cha and Y. Date, Possible involvement of food texture in insulin resistance and energy metabolism in male rats, *J. Endocrinol.*, 2014, **222**, 61-72.
21. D. Su, R. Zhang, F. Hou, J. Chi, F. Huang, S. Yan, L. Liu, Y. Deng, Z. Wei and M. Zhang, Lychee pulp phenolics ameliorate hepatic lipid accumulation by reducing miR-33 and miR-122 expression in mice fed a high-fat diet, *Food Funct.*, 2017, **8**, 808-815.
22. L. Baselga-Escudero, C. Blade, A. Ribas-Latre, E. Casanova, M. J. Salvado, L. Arola and A. Arola-Arnal, Grape seed proanthocyanidins repress the hepatic lipid regulators miR-33 and miR-122 in rats, *Mol. Nutr. Food Res.*, 2012, **56**, 1636-1646.